Fibroblasts positive for meflin have anti-fibrotic properties in pulmonary fibrosis

Yoshio Nakahara[1,12], Naozumi Hashimoto[1,12], Koji Sakamoto[1,12], Atsushi Enomoto[2], Taylor S. Adams[3], Toyoharu Yokoi[4], Norihito Omote[1,3], Sergio Poli[5], Akira Ando[1], Keiko Wakahara[1], Atsushi Suzuki[1], Masahide Inoue[1], Akitoshi Hara[2,6], Yasuyuki Mizutani[2,7], Kazuyoshi Imaizumi[8], Tsutomu Kawabe[9], Ivan O. Rosas[10], Masahide Takahashi[2], Naftali Kaminski[3] and Yoshinori Hasegawa[11]

[1]Dept of Respiratory Medicine, Nagoya University Graduate School of Medicine, Nagoya, Japan. [2]Dept of Pathology, Nagoya University Graduate School of Medicine, Nagoya, Japan. [3]Section of Pulmonary, Critical Care and Sleep Medicine, Yale School of Medicine, New Haven, CT, USA. [4]Dept of Pathology, Tsushima City Hospital, Tsushima, Japan. [5]Dept of Medicine, Mount Sinai Medical Center, Miami Beach, FL, USA. [6]Dept of Cardiology, Nagoya University Graduate School of Medicine, Nagoya, Japan. [7]Dept of Gastroenterology and Hepatology, Nagoya University Graduate School of Medicine, Nagoya, Japan. [8]Dept of Respiratory Medicine, Fujita Health University, Toyoake, Japan. [9]Dept of Pathophysiological Laboratory Sciences, Nagoya University Graduate School of Medicine, Nagoya, Japan. [10]Dept of Medicine, Section of Pulmonary, Critical Care and Sleep Medicine, Baylor College of Medicine, Houston, TX, USA. [11]National Hospital Organization Nagoya Medical Center, Nagoya, Japan. [12]These authors contributed equally to this work.

Corresponding author: Naozumi Hashimoto (hashinao@med.nagoya-u.ac.jp)

Shareable abstract (@ERSpublications)
Fibroblastic foci are the pathological hallmark lesions in idiopathic pulmonary fibrosis. This study identified a novel population of fibroblasts positive for meflin in fibroblastic foci. Fibroblasts positive for meflin had anti-fibrotic properties. https://bit.ly/3fabMo6

Cite this article as: Nakahara Y, Hashimoto N, Sakamoto K, *et al*. Fibroblasts positive for meflin have anti-fibrotic properties in pulmonary fibrosis. *Eur Respir J* 2021; 58: 2003397 [DOI: 10.1183/13993003.03397-2020].

This article has supplementary material available from erj.ersjournals.com

Received: 15 April 2020
Accepted: 7 May 2021

Abstract

The prognosis of elderly individuals with idiopathic pulmonary fibrosis (IPF) remains poor. Fibroblastic foci, in which aggregates of proliferating fibroblasts and myofibroblasts are involved, are the pathological hallmark lesions in IPF to represent focal areas of active fibrogenesis. Fibroblast heterogeneity in fibrotic lesions hampers the discovery of the pathogenesis of pulmonary fibrosis. Therefore, to determine the pathogenesis of IPF, identification of functional fibroblasts is warranted. The aim of this study was to determine the role of fibroblasts positive for meflin, identified as a potential marker for mesenchymal stromal cells, during the development of pulmonary fibrosis.

We characterised meflin-positive cells in a single-cell atlas established by single-cell RNA sequencing (scRNA-seq)-based profiling of 243 472 cells from 32 IPF lungs and 29 normal lung samples. We determined the role of fibroblasts positive for meflin using bleomycin (BLM)-induced pulmonary fibrosis.

scRNA-seq combined with *in situ* RNA hybridisation identified proliferating fibroblasts positive for meflin in fibroblastic foci, not dense fibrosis, of fibrotic lungs in IPF patients. A BLM-induced lung fibrosis model for meflin-deficient mice showed that fibroblasts positive for meflin had anti-fibrotic properties to prevent pulmonary fibrosis. Although transforming growth factor-β-induced fibrogenesis and cell senescence with the senescence-associated secretory phenotype were exacerbated in fibroblasts *via* the repression or lack of meflin, these were inhibited in meflin-deficient fibroblasts with meflin reconstitution.

These findings provide evidence to show the biological importance of meflin expression on fibroblasts and myofibroblasts in the active fibrotic region of pulmonary fibrosis.

Introduction

Although clinical advances have been made in pharmacotherapeutic approaches to idiopathic pulmonary fibrosis (IPF) [1], the prognosis of elderly individuals with IPF remains poor with a 5-year survival rate worse than several types of cancer [2]. Although the pathogenesis of IPF remains unclear, some studies on pulmonary fibrosis suggest the potential role of ageing-related responses such as cell senescence in fibroblasts and epithelial cells [3, 4]. The pathological hallmark lesions in IPF comprise fibroblastic foci in

fibrotic lesions that may progress to dense fibrosis [5, 6]. Fibroblastic foci have been assumed to represent focal areas of active fibrogenesis, in which aggregates of proliferating fibroblasts and myofibroblasts are involved [7]. As fibroblasts isolated from IPF lungs have heterogenous phenotypes and properties different from those of normal lung fibroblasts [8, 9], their diversity makes it difficult to understand the pathogenesis of pulmonary fibrosis [10–14]. Therefore, to determine the pathogenesis of IPF, identification of functional fibroblasts is warranted.

The advent of single-cell RNA sequencing (scRNA-seq), which enables us to detect well-known or new cell populations without any reliable surface markers [15], has recently identified a new "ionocyte" cell type in the conducting airway epithelium [16, 17]. Although scRNA-seq technologies have successfully defined heterogeneity within cell populations in fibrotic lungs during the development of pulmonary fibrosis [18–21], they have not fully identified a novel and functional population of fibroblasts with a fibrogenic or anti-fibrogenic phenotype from the fibrotic lungs of IPF patients.

Although meflin (also known as immunoglobulin superfamily containing leucine-rich repeat (ISLR)) has recently been identified as a potential marker for mesenchymal stromal cells such as fibroblasts and pericytes [22], the characterisation of fibroblasts positive for meflin has not been fully determined in normal or fibrotic lungs. Whether fibroblasts positive for meflin play a critical role during the development of pulmonary fibrosis also remains unknown.

The aim of this study was to determine the role of fibroblasts positive for meflin during the development of pulmonary fibrosis.

Material and methods

A detailed description of the methods is provided in the supplementary material.

Analysis of microarray data of human samples

We analysed Gene Expression Omnibus (www.ncbi.nlm.nih.gov/geo) dataset GSE47460-GPL14550 for ISLR transcript levels in normal lungs and lungs of IPF patients. Log_2-transformed normalised expression values for the ISLR gene in 122 IPF lungs and 91 control lungs were retrieved using GEO2R and visualised using Prism version 7 (GraphPad, San Diego, CA, USA).

Sample preparation for single-cell sequencing

IPF lungs were obtained from patients undergoing transplants, while healthy lungs comprised rejected donor lung organs that underwent lung transplantation at the Brigham and Women's Hospital (Boston, MA, USA) or donor organs provided by the National Disease Research Interchange (https://ndriresource.org). The study protocol was approved by the Partners Healthcare Institutional Board Review (protocol 2011P002419). Details of sample preparation and subsequent scRNA-seq methodology have been presented elsewhere [23].

Sample preparation in the CHILDREN registry

Human lung tissue samples from 10 patients with IPF and five subjects with normal lungs were obtained *via* surgical lung biopsy or remnants of lung resection at Nagoya University Hospital (Nagoya, Japan). All study subjects were enrolled in the CHILDREN registry (CHronic Interstitial Lung Disease REgistry of Nagoya University), as approved by the Nagoya University Ethics Committee (approval date 20 December 2018; approval 2017-0169-3).

Mouse fibrosis model

Pulmonary fibrosis was induced by endotracheal bleomycin (BLM) injection as previously described [10, 11]. All animal studies were reviewed and approved by the University Committee on Use and Care of Animals at Nagoya University Graduate School of Medicine (approval date 22 March 2019; approval 31333).

Statistical analysis

Data are presented as median±range when specified. Comparison of two groups was performed using the unpaired t-test (parametric) or Mann–Whitney U-test (nonparametric). For multiple comparisons, we used repeated measures ANOVA with *post hoc* Bonferroni's test or one-way ANOVA with *post hoc* Tukey's test to determine the significance. Kaplan–Meier survival estimation with a log-rank test was performed to compare the animal survival rate between treatment groups. All statistical analyses were performed using SPSS statistical software (IBM, Armonk, NY, USA). A p-value <0.05 was considered statistically significant.

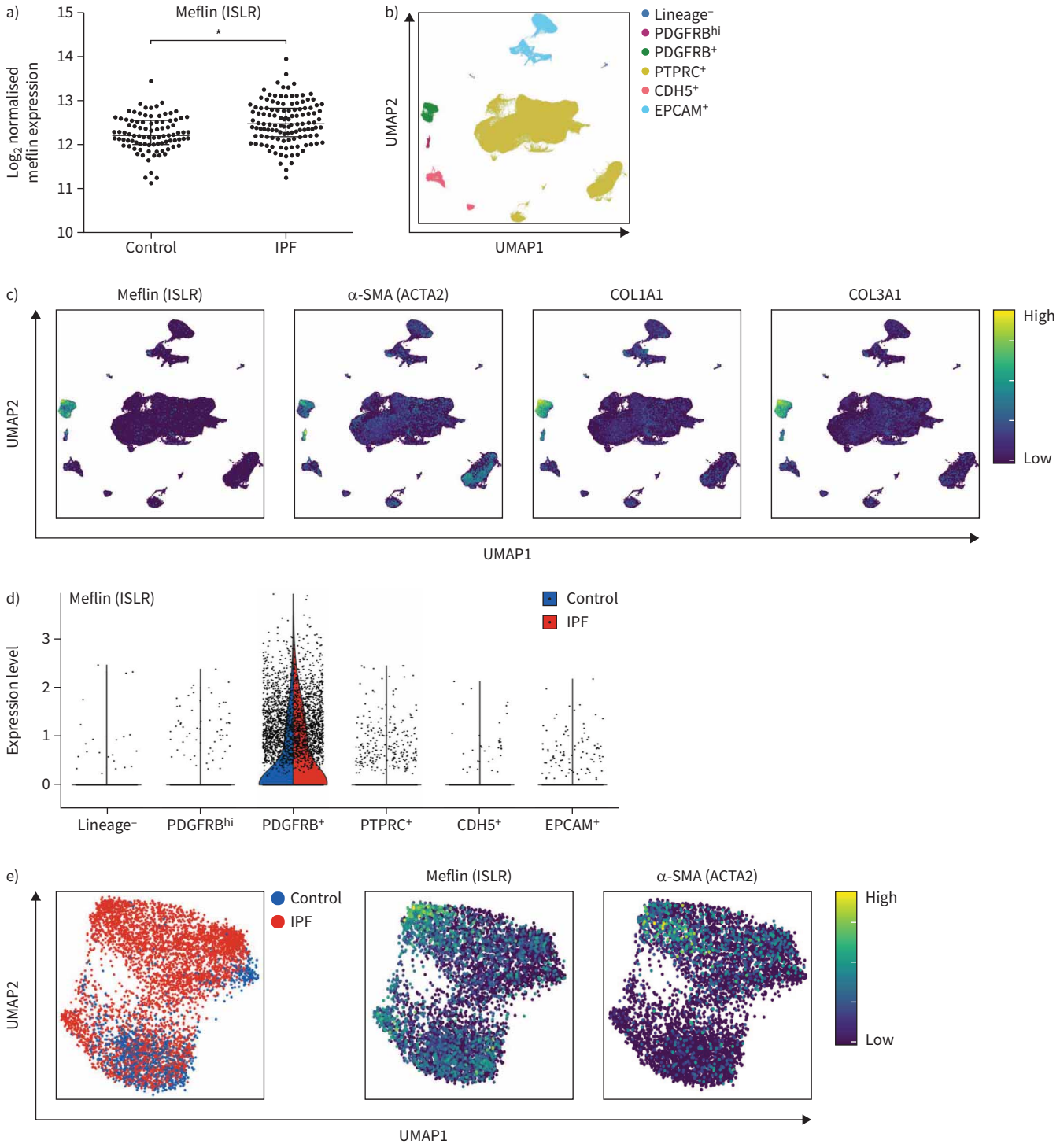

FIGURE 1 Analysis of ISLR expression in human lung single-cell RNA sequencing data. a) Normalised expression of ISLR mRNA in lung homogenates from idiopathic pulmonary fibrosis (IPF) (n=122) and control (n=91) lungs. Data were obtained from the published Gene Expression Omnibus microarray dataset (GSE47460-GPL14550). *: p<0.0001 (Mann–Whitney U-test between two variables). b) Labelling of clusters stratified according to the expression of classical cell markers by Uniform Manifold Approximation and Projection (UMAP): immune (PTPRC), epithelial (EPCAM), vascular (CDH5) and mesenchymal (PDGFRB) cell populations. c) Feature plots showing normalised gene expression of ISLR and other genes relevant to lung fibrosis (ACTA2, COL1A1 and COL3A1). d) Violin plots showing expression of ISLR is restricted to the PDGFRB^{+} cluster. e) Distribution of ISLR expression within the PDGFRB^{+} cluster. The left panel indicates the origins of the cells stratified by disease state (control or IPF); the middle and right panels indicate the expression levels of ISLR and ACTA2, respectively. α-SMA: α-smooth muscle actin.

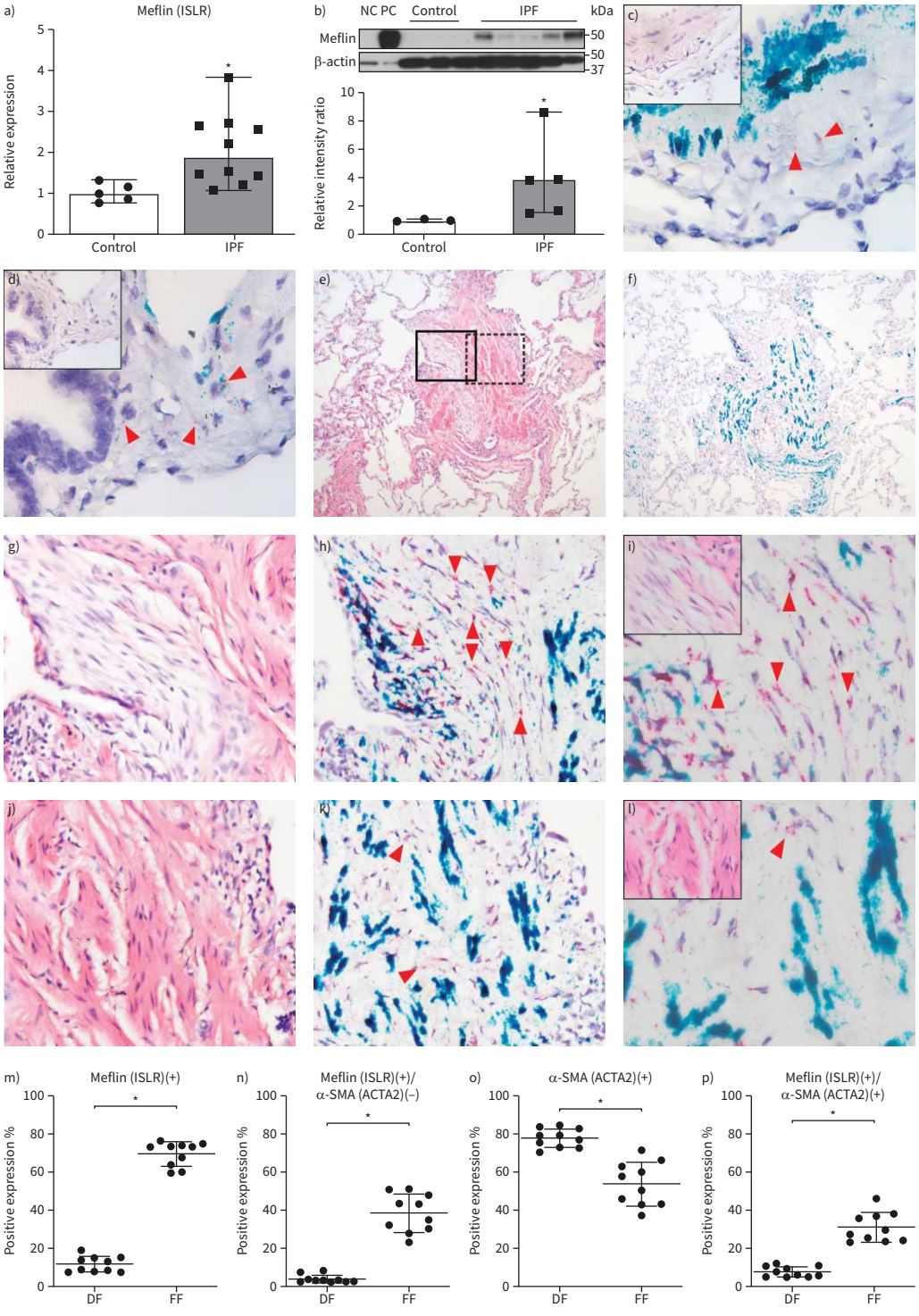

FIGURE 2 Meflin expression in lung tissues from healthy subjects and patients with idiopathic pulmonary fibrosis (IPF). a) Expression of ISLR transcripts was evaluated in lung homogenates from IPF (n=10) and control (n=5) lungs among subjects enrolled in the CHILDREN registry. *: p<0.05 *versus* control. b) Meflin protein expression was evaluated in lung fibroblasts derived from IPF (n=5) and control (n=3) lungs among subjects enrolled in the CHILDREN registry. *: p<0.05 *versus* control. c, d) *In situ* hybridisation (ISH) for ISLR (red) and ACTA2 (green) and haematoxylin/eosin (HE) staining (inset) are shown for the c) lined and d) dashed box areas in supplementary figure S3e. Original magnification: ×400. e, f) HE staining and ISH for ISLR (red) and ACTA2 (green) were performed for representative lung sections from the IPF group (case 193). Original magnification: ×40. The lined and dashed box areas in (e) indicate fibrotic foci region and dense fibrosis region, respectively.

HE staining is shown for the g) lined and j) dashed box areas, respectively. Original magnification: ×200. ISH for ISLR (red) and ACTA2 (green) is also shown for the h) lined and k) dashed box areas, respectively. Original magnification: ×200. HE staining (inset) and ISH for ISLR (red) and ACTA2 (green) are shown for the lined i) and l) dashed box areas, respectively. Original magnification: ×400. Red arrowheads (h, i, k and l) indicate meflin-positive cells. m–p) Percentage of ISLR- and/or ACTA2-positive cells that colocalised with nuclei in dense fibrosis (DF) and fibrotic foci (FF). *: p<0.05 *versus* DF. a, b, m–p) Mann–Whitney U-test. NC: negative control (cell lysate of 293FT cells); PC: positive control (cell lysate of 293FT cells stably expressing human ISLR); α-SMA: α-smooth muscle actin.

Results

Bulk and single-cell transcriptome profiling for characterisation of meflin-expressing cells in normal and IPF lungs

In our previously published microarray dataset, we found that the expression of ISLR mRNA, which encodes meflin protein, was significantly increased in lung homogenate from IPF lungs compared with control lungs in the GSE47460 dataset from the Lung Genomics Research Consortium (figure 1a). To explore the expression profile of ISLR within lung cells of various lineages, we analysed single-cell transcriptomes of 243 472 cells from 29 normal lung samples and 32 IPF lungs. The analysis with Uniform Manifold Approximation and Projection (UMAP) showed 38 different clusters of cells. Visualisation of expression levels with classical markers of cell lineage including immune (protein tyrosine phosphatase receptor type C (PTPRC)), epithelial (epithelial cell adhesion molecule (EPCAM)), vascular (cadherin 5 (CDH5)) and stromal (platelet derived growth factor receptor β (PDGFRB)) cell types validated that each cluster had distinct gene expression profiles (figure 1b and supplementary figure S1a). We roughly stratified the identified clusters into six groups according to the observed expression of these classical lineage markers (figure 1b). In this dataset, the expression of ISLR appeared to be abundant and almost restricted to the PDGFRB$^+$/EPCAM$^-$/CDH5$^-$/PTPRC$^-$ group (hereafter the PDGFRB$^+$ group) (figure 1c and d, supplementary figure S1b–e and supplementary table S1), which is assumed to include fibroblasts and myofibroblasts by expression of distinct markers, further supported by visualisation of positive expression for ACTA2, COL1A1 and COL3A1 (figure 1c). When we investigated the PDGFRB$^+$ group, we further identified two subgroups (figure 1e). One subgroup consisted of cells from both normal lungs and IPF lungs with scarce expression in ACTA2, the other consisted largely of IPF-derived cells and was frequently positive for ACTA2 expression (figure 1e). ISLR-positive cells were observed in both subgroups (figure 1e). Analysis of ISLR expression profiles in single-cell resolution using a user-friendly web database (IPF Cell Atlas; http://ipfcellatlas.com) validated its distinct expression in the stromal cell lineage (supplementary figure S2).

To estimate the function of ISLR-positive stromal cells in normal and disease lung states, we characterised the profiles of genes coordinately expressed with ISLR. We found a set of genes with significant positive correlations with ISLR levels in the PDGFRB$^+$ population (supplementary figure S1f), which included typical fibrosis markers such as COL1A1 (ρ=0.312, false discovery rate (FDR) p=4.726E-118), COL3A1 (ρ=0.286, FDR p=1.35E-98), POSTN (ρ=0.220, FDR p=3.056E-57) and FN1 (ρ=0.1792, FDR p=1.084E-37). We further stratified cells by lung condition (control lungs or IPF lungs) and conducted gene enrichment analysis of the top 400 genes with positively correlated ISLR expression (supplementary figure S1g) using GeneGo MetaCore software (https://clarivate.com/products/metacore). Process networks such as “cell adhesion” and “proteolysis” were enriched by ISLR-correlated genes in PDGFRB$^+$ cells from both normal and IPF lungs, suggesting their shared functions of ISLR$^+$ stromal cells in normal and disease settings. Meanwhile, distinct process networks were also highlighted between normal and IPF fibroblasts. For example, ISLR-correlated genes were more enriched in the “proteolysis” process in control lung fibroblasts, while in IPF fibroblasts, processes relevant to “cytoskeleton” processes were enriched (supplementary figure S1g).

Taken together, these results suggest that ISLR expression is restricted in a cluster of stromal cell lineage in human lungs and is often coexpressed with fibrotic genes such as ACTA2, COL1A1 and COL3A1 (figure 1c). ISLR-positive cells with ACTA2$^+$ appear increased, particularly in cases of IPF. Gene enrichment analysis of coordinately expressed genes with ISLR implies the functional characteristics of ISLR$^+$ cells, with highlighted cellular processes such as matrix remodelling and cell–matrix interaction.

ISLR expression in lung tissues from healthy subjects and patients with IPF

We determined localisation of meflin in lung tissues from five subjects with normal lungs (the control group) and 10 patients with pathologically diagnosed IPF (the IPF group) among subjects enrolled in the

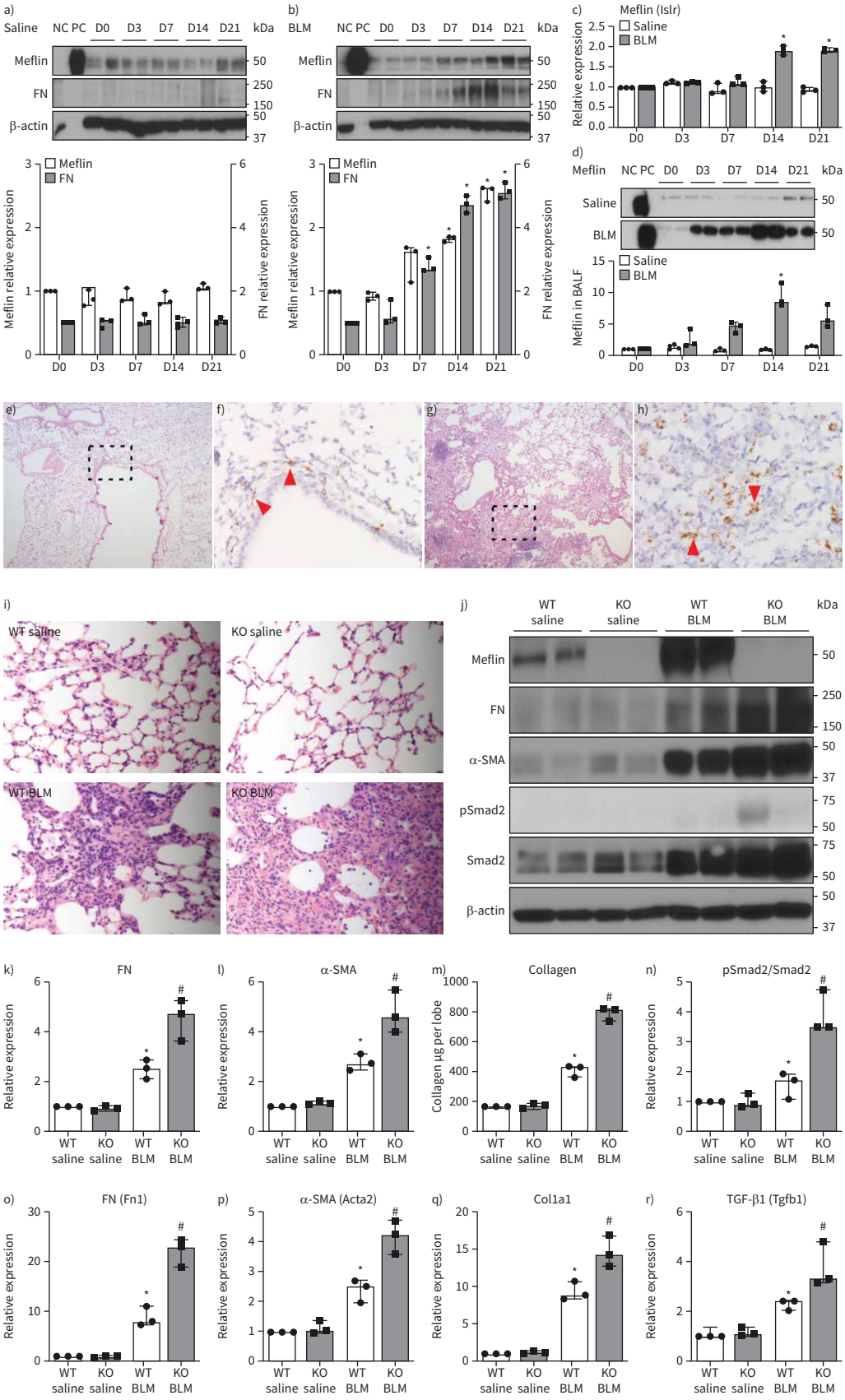
a)
Saline
NC PC D0 D3 D7 D14 D21 kDa
Meflin
FN
β-actin
50
250
150
50
37
Meflin
FN
Meflin relative expression
FN relative expression
D0 D3 D7 D14 D21
b)
BLM
NC PC D0 D3 D7 D14 D21 kDa
Meflin
FN
β-actin
50
250
150
50
37
Meflin
FN
Meflin relative expression
FN relative expression
D0 D3 D7 D14 D21
c)
Meflin (Islr)
Saline
BLM
Relative expression
D0 D3 D7 D14 D21
d)
Meflin
NC PC D0 D3 D7 D14 D21 kDa
Saline
BLM
50
50
Saline
BLM
Meflin in BALF
D0 D3 D7 D14 D21
e)
f)
g)
h)
i)
WT saline
KO saline
WT BLM
KO BLM
j)
WT saline
KO saline
WT BLM
KO BLM
kDa
Meflin
FN
α-SMA
pSmad2
Smad2
β-actin
50
250
150
50
37
75
50
75
50
50
37
k)
FN
Relative expression
WT saline
KO saline
WT BLM
KO BLM
l)
α-SMA
Relative expression
m)
Collagen
Collagen μg per lobe
n)
pSmad2/Smad2
Relative expression
o)
FN (Fn1)
Relative expression
p)
α-SMA (Acta2)
Relative expression
q)
Col1a1
Relative expression
r)
TGF-β1 (Tgfb1)
Relative expression

FIGURE 3 Anti-fibrotic effect of meflin-positive fibroblasts in an *in vivo* bleomycin (BLM)-induced lung fibrosis model. Western blot analyses of meflin, fibronectin (FN) and β-actin in lung homogenates from a) saline- and b) BLM-treated mice at the indicated time (days (D)) were performed. A representative blot is shown in the upper panels. Intensity of expression was evaluated and is shown after normalisation to β-actin expression in the lower panels. *: p<0.05 *versus* D0. c) Real-time PCR analyses for Islr were performed for lung homogenates from saline- and BLM-treated mice collected at the indicate time. *: p<0.05 *versus* D0. d) Western blot analyses of meflin was performed for bronchoalveolar lavage fluid (BALF) supernatants (2 µg total protein per sample) from saline- and BLM-treated mice at the indicated time. A representative blot is shown in the upper panel. Intensity of expression was evaluated and is shown in the lower panel. *: p<0.05 *versus* D0. e–h) Representative lung sections from e, f) saline- and g, h) BLM-treated mice were examined by e, g) haematoxylin/eosin and f, h) *in situ* hybridisation (ISH) for Islr (brown). Dashed box areas in e) and g) indicate the periepithelial region and fibrotic region, respectively. Red arrowheads in f) and h) indicate Islr-positive cells. Original magnification: ×200. i) The BLM-induced lung fibrosis model was applied to wild-type (WT) and meflin-deficient (knockout (KO)) mice (WT saline n=6, KO saline n=6, WT BLM n=9 and KO BLM n=9). Representative histological sections of lung tissue obtained at day 14 following BLM or saline challenge in WT and KO mice. Original magnification: ×200. j) Representative blots from Western blot analyses of meflin, FN, α-smooth muscle actin (α-SMA), phosphorylated Smad2 (pSmad2), Smad2 and β-actin in lung homogenates from saline- and BLM-treated mice. k, l) Intensity of expression of k) FN and l) α-SMA was evaluated and is shown after normalisation to β-actin expression. m) Collagen content evaluated by Sircol collagen assay. n) Ratio of pSmad2 to Smad2 presented as the intensity level. o–r) Real-time PCR analyses for o) Fn1, p) Acta2, q) Col1a1 and r) Tgfb1 for lung homogenates from treated mice. *: p<0.05 *versus* saline-treated WT mice. #: p<0.05 *versus* BLM-treated WT mice. a–d) Repeated measures ANOVA with *post hoc* Bonferroni's test; i) log-rank test; k–r) one-way ANOVA with *post hoc* Tukey's test. Experiments were repeated three times with similar results. NC: negative control (cell lysate of 293FT cells); PC: positive control (cell lysate of 293FT cells stably expressing mouse Islr); TGF-β: transforming growth factor-β.

CHILDREN registry. Patient characteristics are shown in supplementary table S2. The levels of ISLR mRNA expression were significantly higher in lung homogenates from the IPF group than in those from the control group (figure 2a). The IPF group also showed significant increases in FN1, ACTA2 and COL1A1 mRNA expression compared with the control group (supplementary figure S3a–c). The levels of meflin protein and ISLR mRNA expression were significantly higher in lung fibroblasts derived from the IPF group than in those from the control group (figure 2b and supplementary figure S3d). Dual *in situ* hybridisation (ISH) for ISLR (meflin) and ACTA2 (α-smooth muscle actin (α-SMA)) was performed (figure 2c–l and supplementary figures S4–S6). A previous ISH study suggests that the expression of ISLR is localised in subendothelial or perivascular resident fibroblasts in the bone marrow, adipose tissue and other organs [22]. ISLR expression was not detected in epithelial, endothelial or alveolar macrophages in normal lungs (figure 2c and d, and supplementary figure S3e). Although ISLR-positive fibroblasts were sporadically distributed and scattered in the perivascular region (shown by a lined box in supplementary figure S3e and figure 2c) or periepithelial region (shown by a dashed box in supplementary figure S3e and figure 2d), these cells appeared not to be positive for ACTA2 (figure 2c and d). The lung specimens from 10 patients with IPF were also evaluated by dual ISH for ISLR and ACTA2 (figure 2e–l and supplementary figures S4–S6). The ISH study demonstrated increasing numbers of ISLR-positive fibroblasts were observed in the lesions of fibroblastic foci (shown by a lined box in figure 2e and f–i). Meanwhile, most fibroblasts in the lesions of dense fibrosis (shown by a dashed box in figure 2e, f and j–l) were myofibroblasts with ACTA2 mRNA expression and only a few ISLR-positive fibroblasts were scattered. When double staining for ISLR and E-cadherin was performed in fibrotic lung tissues, ISLR mRNA expression was not observed in the cells positive for E-cadherin (supplementary figure S3f–i). The proportions of ISLR- and/or ACTA2-positive fibroblasts were manually quantified in the lesions of fibroblastic foci and dense fibrosis among 10 patients with IPF (figure 2m–p). The ISH analysis demonstrated that >70% of fibroblasts were positive for ISLR in the lesions of fibroblastic foci, ∼50% of which were negative for ACTA2 (figure 2m and n). In dense fibrotic lesions, >70% of fibroblasts were ACTA2-positive myofibroblasts; >95% of myofibroblasts were negative for ISLR (figure 2o and p).

Anti-fibrotic effect of meflin-positive fibroblasts in an in vivo *BLM-induced lung fibrosis model*

To evaluate the longitudinal expression of meflin during the development of lung fibrosis, BLM-induced lung fibrosis was established in C57BL/6J (wild-type (WT)) mice [10, 11, 24]. Western blotting showed that meflin protein expression increased in a time-dependent manner in BLM-treated lungs, but not in saline-treated lungs, followed by *de novo* fibronectin protein expression (figure 3a and b). Real-time PCR showed that the endogenous Islr transcripts were significantly induced in the fibrotic phase during the development of pulmonary fibrosis, accompanied by the increasing expression of fibrogenic variables (figure 3c and supplementary figure S7a–f). Next, we determined whether soluble meflin could be detected in bronchoalveolar lavage (BAL) supernatants. Western blotting showed that a significant increase in *de novo* soluble meflin expression was observed in BAL supernatants from BLM-treated lungs compared with those from saline-treated lungs (figure 3d). The ISH study for Islr showed that Islr-positive fibroblasts were sporadically distributed and scattered in perivascular or periepithelial regions of the normal

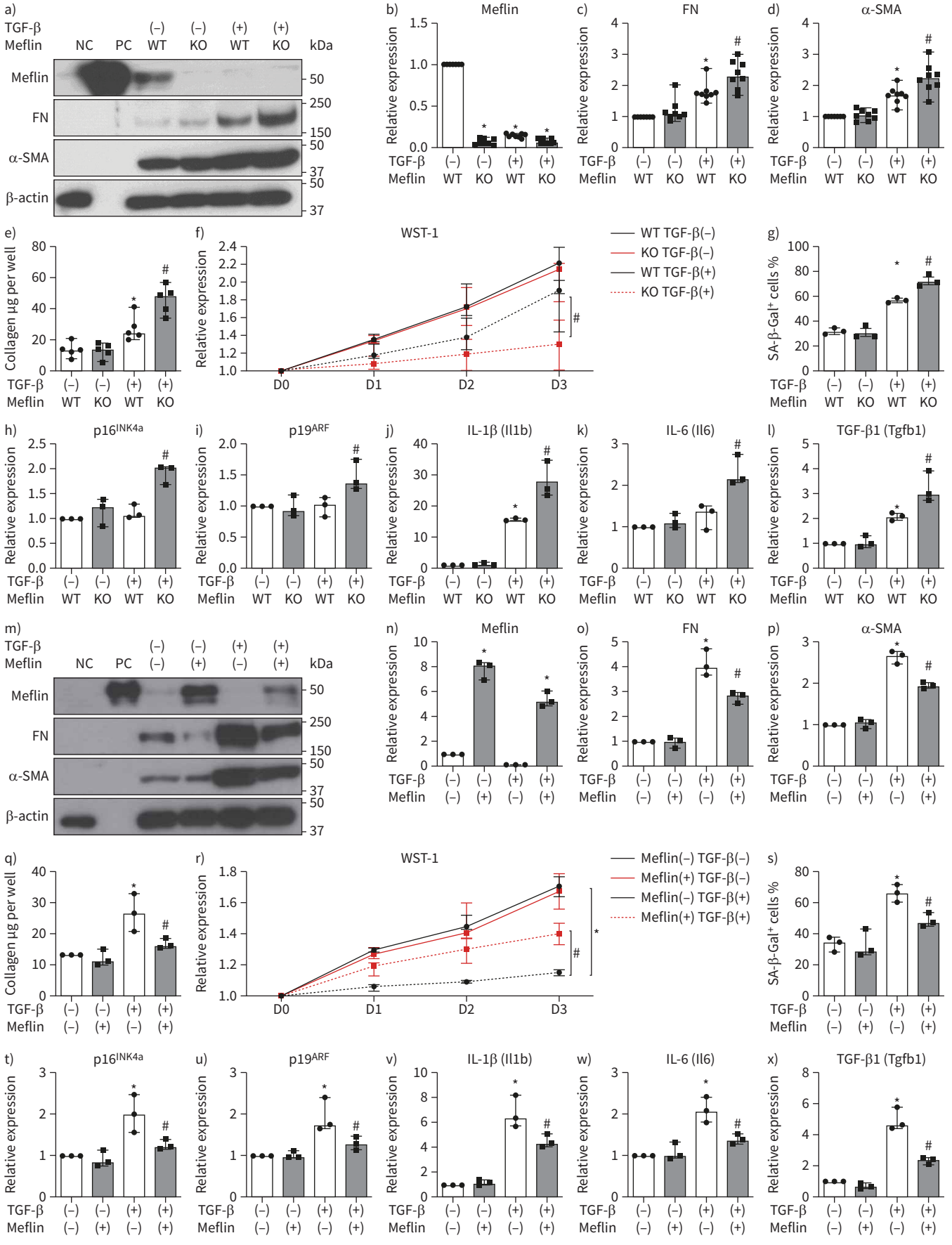
a)
TGF-β
Meflin
NC
PC
(–) WT
(–) KO
(+) WT
(+) KO
kDa
Meflin
FN
α-SMA
β-actin
50
250
150
50
37
50
37
b) Meflin
c) FN
d) α-SMA
Relative expression
e) Collagen μg per well
f) WST-1
WT TGF-β(–)
KO TGF-β(–)
WT TGF-β(+)
KO TGF-β(+)
D0
D1
D2
D3
g) SA-β-Gal+ cells %
h) p16INK4a
i) p19ARF
j) IL-1β (Il1b)
k) IL-6 (Il6)
l) TGF-β1 (Tgfb1)
m)
n) Meflin
o) FN
p) α-SMA
q) Collagen μg per well
r) WST-1
Meflin(–) TGF-β(–)
Meflin(+) TGF-β(–)
Meflin(–) TGF-β(+)
Meflin(+) TGF-β(+)
s) SA-β-Gal+ cells %
t) p16INK4a
u) p19ARF
v) IL-1β (Il1b)
w) IL-6 (Il6)
x) TGF-β1 (Tgfb1)

FIGURE 4 Anti-fibrotic roles of meflin in primary mouse lung fibroblasts *ex vivo* against transforming growth factor (TGF)-β-induced fibrogenesis. a) Western blot analyses of meflin, fibronectin (FN) and α-smooth muscle actin (α-SMA) in control or TGF-β-stimulated primary lung wild-type (WT) and knockout (KO) fibroblasts were performed. A representative blot is shown. b–d) Intensity of expression of b) meflin, c) FN and d) α-SMA was evaluated and is shown after normalisation to β-actin expression. e) Collagen content of cell lysate evaluated by Sircol collagen assay. f) A WST-1 assay was performed for control or TGF-β-stimulated primary lung fibroblasts from WT and KO mice. g) Numbers of senescence-associated β-galactosidase (SA-β-Gal)-positive cells were also evaluated in control or TGF-β-stimulated primary lung fibroblasts from WT and KO mice. h–l) Real-time PCR analyses for h) $p16^{INK4a}$, i) $p19^{ARF}$, j) Il1b, k) Il6 and l) Tgfb1 were performed in control or TGF-β-stimulated primary lung fibroblasts from WT and KO mice. *: p<0.05 *versus* control-stimulated fibroblasts from WT mice; #: p<0.05 *versus* TGF-β-stimulated fibroblasts from WT mice. m) Western blot analyses of meflin, FN and α-SMA in control or TGF-β-stimulated primary lung KO fibroblasts, for which control or meflin were reconstituted by using lentivirus, were performed. A representative blot is shown. n–p) Intensity of expression of n) meflin, o) FN and p) α-SMA was evaluated and is shown after normalisation to β-actin expression. q) Collagen content of cell lysate evaluated by Sircol collagen assay. r) A WST-1 assay was performed for these cells. s) Numbers of SA-β-Gal-positive cells were also evaluated. t–x) Real-time PCR analyses for t) $p16^{INK4a}$, u) $p19^{ARF}$, v) Il1b, w) Il6 and x) Tgfb1 were also performed in control or TGF-β-stimulated primary lung fibroblasts from KO mice, for which control or meflin were reconstituted. *: p<0.05 *versus* control-stimulated KO fibroblasts with control gene induction; #: p<0.05 *versus* with TGF-β-stimulated KO fibroblasts with control gene induction. f, r) Repeated measures ANOVA with *post hoc* Bonferroni's test; b–e, g–l, n–q, s–x) one-way ANOVA with *post hoc* Tukey's test. Experiments were repeated at least three times with similar results. NC: negative control (cell lysate of 293FT cells); PC: positive control (cell lysate of 293FT cells stably expressing mouse Islr); D: days; IL: interleukin.

mouse lungs, while increasing numbers of Islr-positive cells were observed in the fibrotic lesions on BLM at day 14 (figure 3e–h and supplementary figure S7g–n). To evaluate the role of meflin expression during the development of pulmonary fibrosis, the BLM-induced lung fibrosis model was applied to meflin-deficient (knockout (KO)) mice. Lungs from BLM-treated KO mice exhibited more severe pulmonary fibrosis compared with those from BLM-treated WT mice (figure 3i). Western blotting and a Sircol collagen assay were performed using lung homogenates from BLM-treated and saline-treated groups at day 14 (figure 3j–n). Although the saline KO group did not show an increase in fibronectin and α-SMA protein expression, collagen content or Smad2 activation compared with the saline WT group, the expression of fibronectin and α-SMA protein, collagen content, and Smad2 activation were significantly higher in the BLM KO group than in the BLM WT group (figure 3j–n). Real-time PCR showed that *de novo* expression of fibrogenic variables including Fn1, Acta2, Col1a1 and Tgfb1, and the related mediators, was significantly induced in the BLM KO mice compared with those in the BLM WT mice (figure 3o–r and supplementary figure S7o–z). Taken together, these data clearly suggest a protective role of meflin *via* anti-fibrotic effects against the development of BLM-induced lung fibrosis *in vivo*.

Anti-fibrotic roles of meflin in primary lung fibroblasts ex vivo *against transforming growth factor-β-induced fibrogenesis*

Our survey of different cell types suggested that meflin was detected in lung fibroblasts, but not in other cells, including epithelial, endothelial and peripheral blood mononuclear cells (supplementary figure S3j and k), compatible with a previous study [22]. When naïve primary lung fibroblasts were isolated from WT mice (WT fibroblasts) and meflin KO mice (KO fibroblasts), both cells showed mostly typical spindle-shaped fibroblast morphology (data not shown). The effects of meflin on transforming growth factor (TGF)-β-induced phenotypes in fibroblasts were evaluated by Western blotting, Sircol collagen assay and real-time PCR (figure 4a–e, and supplementary figure S8a–f and h–j). Although primary WT fibroblasts showed meflin protein expression, TGF-β stimulation for 48 h led to a <80% decrease in meflin expression in the cells (figure 4a and b, and supplementary figure S8a). The data showed that when no TGF-β was added, KO fibroblasts did not show *de novo* induction of fibronectin, α-SMA or collagen with Smad activation compared with WT fibroblasts (figure 4a and c–e, and supplementary figure S8b–f). When these KO fibroblasts were treated with TGF-β, significant increases in fibronectin, α-SMA and collagen expression with Smad activation were observed compared with WT fibroblasts (figure 4a and c–e, and supplementary figure S8b–f). To evaluate the effect of meflin on proliferation ability in fibroblasts, a WST-1 cell proliferation assay and cell count was performed (figure 4f and supplementary figure S8g). Both WT and KO fibroblasts showed similar proliferation ability when no TGF-β was added. Although WT fibroblasts treated with TGF-β had a slight repression of proliferation compared with fibroblasts without TGF-β, TGF-β-treated KO fibroblasts remarkably showed no or little proliferation, reminiscent of cell senescence [4, 22, 25]. To evaluate senescence-state cells, senescence-associated β-galactosidase (SA-β-Gal) staining was performed for these fibroblasts (figure 4g). Meflin KO fibroblasts treated with TGF-β included a significantly larger number of SA-β-Gal-positive cells when compared with TGF-β-treated WT fibroblasts. Real-time PCR was also performed for relatively reliable cell senescence markers and a senescence-associated secretory phenotype (SASP) such as $p16^{INK4a}$, $p19^{ARF}$, Il1b, Il6 and Tgfb1 expression [4, 25–27]. TGF-β-stimulated KO fibroblasts had significantly increased expression

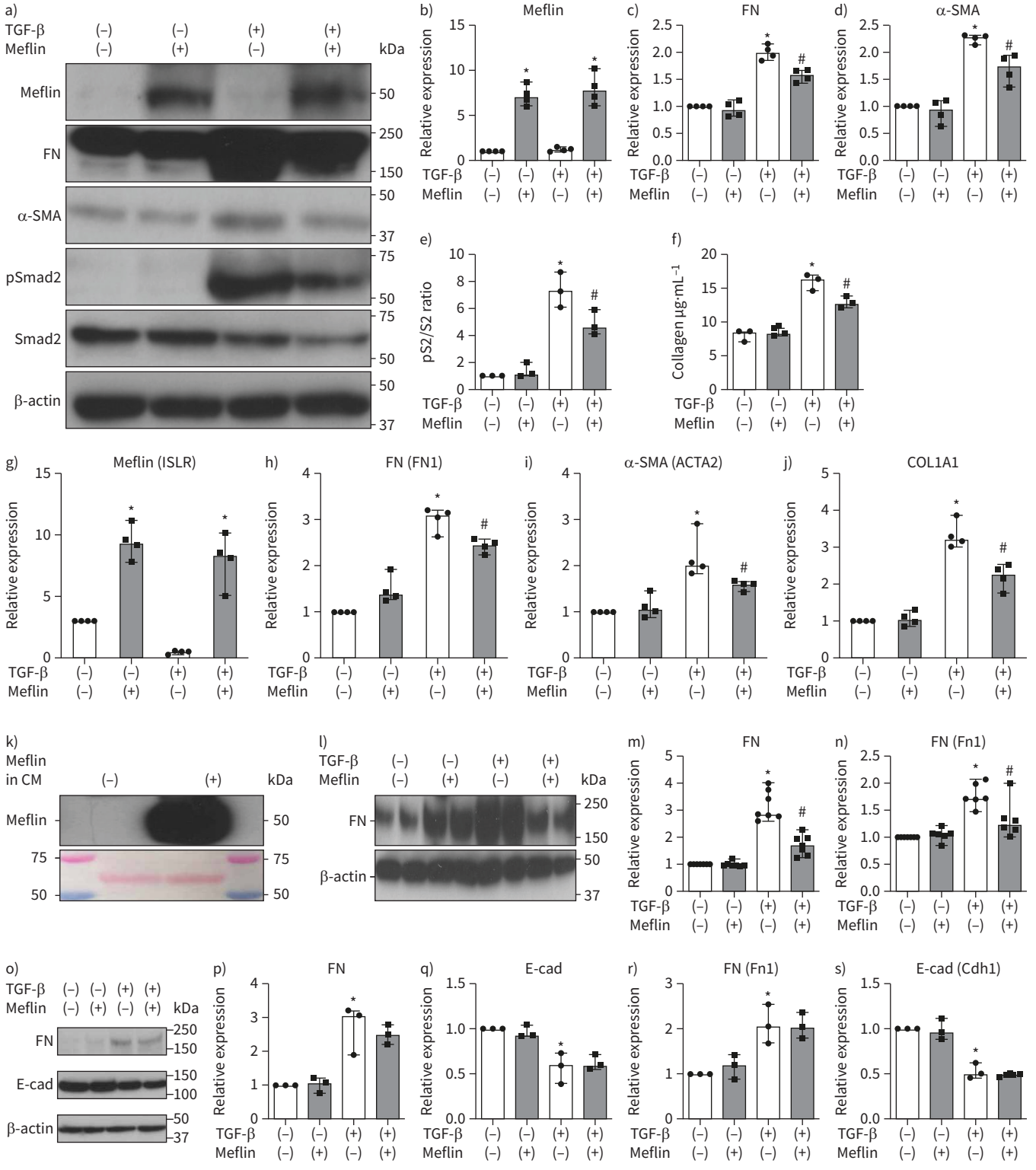

FIGURE 5 Anti-fibrotic effect of meflin in human lung fibroblasts and no anti-fibrotic effect of soluble meflin in epithelial cells against transforming growth factor (TGF)-β-induced fibrogenesis. a) Western blot analyses were performed of meflin, fibronectin (FN), α-smooth muscle actin (α-SMA), phosphorylated Smad2 (pSmad2), Smad2 and β-actin in control or TGF-β-stimulated normal human adult lung fibroblasts (NHLFs), for which control or human meflin were reconstituted by using lentivirus. A representative blot is shown. b–d) Intensity of expression of b) meflin, c) FN and d) α-SMA was evaluated and is shown after normalisation to β-actin expression. e) Ratio of pSmad2 to Smad2 (pS2/S2) presented as the intensity level. f) Collagen content of conditioned medium collected from reconstituted fibroblasts evaluated by Sircol collagen assay. g–j) Real-time PCR analyses for g) ISLR, h) FN1, i) ACTA2 and j) COL1A1 were performed in control or TGF-β-stimulated NHLFs. *: p<0.05 *versus* control-stimulated

NHLFs with control gene induction; #: p<0.05 *versus* TGF-β-stimulated NHLFs with control gene induction. k) Western blot analysis of meflin was performed for culture medium (CM) (10 µg of total protein per sample) from 293FT cells or 293FT cells stably expressing mouse Islr (upper). Ponceau S staining was also performed for total protein normalisation (lower). A representative blot is shown. l) Western blot analyses of FN and β-actin were performed in control or TGF-β-stimulated primary lung knockout (KO) fibroblasts treated with culture medium from 293FT cells or 293FT cells stably expressing mouse Islr. A representative blot is shown. m) Intensity of expression of FN was evaluated and is shown after normalisation to β-actin expression. n) Real-time PCR analysis for Fn1 was also performed for the cells. *: p<0.05 *versus* control-stimulated KO fibroblasts with control culture medium; #: p<0.05 *versus* TGF-β-stimulated KO fibroblasts with control culture medium. o–q) Western blot analyses of FN, E-cadherin (E-cad) and β-actin were performed in control or TGF-β-stimulated mouse epithelial cells (MLE-12 cells) treated with culture medium from 293FT cells or 293FT cells stably expressing mouse Islr. o) Representative blot. p, q) Intensity of expression of p) FN and q) E-cad was evaluated and is shown after normalisation to β-actin expression. r, s) Real-time PCR analyses for r) Fn1 and s) Cdh1 were also performed for the cells. *: p<0.05 *versus* control-stimulated MLE-12 cells with control culture medium; #: p<0.05 *versus* TGF-β-stimulated MLE-12 cells with control culture medium. b–j, m–s) One-way ANOVA with *post hoc* Tukey's test. Experiments were repeated at least three times with similar results.

levels (figure 4h–k and supplementary figure S8h–j). Furthermore, TGF-β-stimulated KO fibroblasts strikingly showed increased induction of autocrine Tgfb1 transcripts compared with TGF-β-stimulated WT fibroblasts (figure 4l) [4, 25, 28]. Thus, the repression of or lack of meflin in fibroblasts led to TGF-β-induced aberrant fibrogenesis and senescence with the SASP. To determine whether meflin expression in fibroblasts is essential for anti-fibrotic effects against TGF-β-induced fibrogenesis and cell senescence, a model of meflin reconstitution was established in KO fibroblasts using lentivirus expressing meflin. The effects of meflin on TGF-β-induced extracellular matrix (ECM) production and α-SMA expression in fibroblasts were evaluated by Western blotting, Sircol collagen assay and real-time PCR

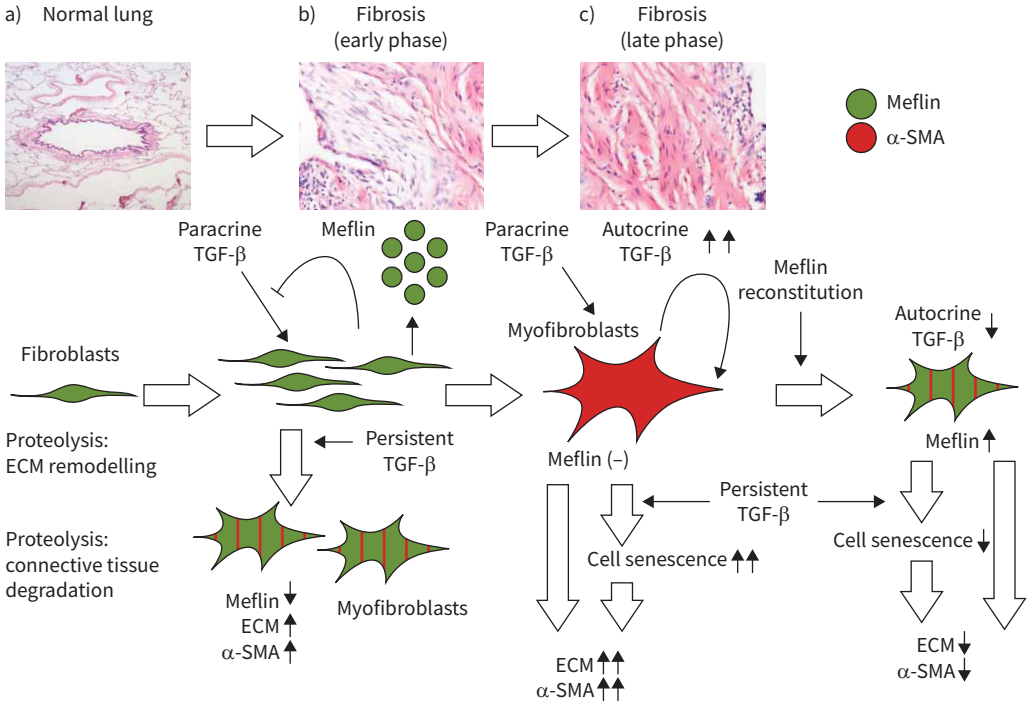

FIGURE 6 A schematic diagram of the anti-fibrotic role of meflin expression on fibroblasts during the development of pulmonary fibrosis. a) In normal lungs, fibroblasts positive for meflin are sporadically distributed in perivascular or periepithelial regions to control extracellular matrix (ECM) homeostasis. b) In the early fibrotic phase, increasing meflin-positive fibroblasts inhibit transforming growth factor (TGF)-β induced fibrogenesis *via* secretion of meflin. Persistent TGF-β stimulation causes loss of meflin expression in fibroblasts and consequently acquisition of *de novo* α-smooth muscle actin (α-SMA) expression and ECM production. c) In the late fibrotic phase, the lack of or repression of meflin in fibroblasts yields TGF-β-induced cellular senescence with a senescence-associated secretory phenotype, accompanied by exacerbation of TGF-β-induced fibrogenesis. Reconstitution of meflin expression in myofibroblasts inhibits TGF-β-induced fibrogenesis and cell senescence.

(figure 4m–q and supplementary figure S8k–p). Lentivirus-mediated transduction of the meflin gene led to the steady expression levels of meflin protein in KO fibroblasts (figure 4m and n, and supplementary figure S8k). Meflin reconstitution successfully repressed *de novo* fibronectin, α-SMA and collagen expression with Smad activation induced by TGF-β (figure 4o–q and supplementary figure S8l–p). The effect of meflin reconstitution on TGF-β-induced senescence with SASP was also evaluated. Repression of cell proliferation induced by TGF-β was significantly restored in the meflin-transduced KO fibroblasts compared with the control transcript-transduced KO fibroblasts (figure 4r and supplementary figure S8q). Significantly decreased numbers of SA-β-Gal-positive cells were also observed in KO fibroblasts with meflin compared with cells with control (figure 4s). These repressive effects of meflin reconstitution against cell senescence were accompanied by the inhibition of the related transcript expression (figure 4t–x and supplementary figure S8r–t). When the anti-fibrotic effect of meflin expression was evaluated in normal human lung fibroblasts using lentivirus expressing meflin, the meflin induction led to the repression of *de novo* fibronectin, α-SMA and collagen expression with Smad activation induced by TGF-β (figure 5a–j). To determine the effect of paracrine meflin on epithelial cells, TGF-β-stimulated lung epithelial cells (MLE-12 cells) were treated with culture medium including soluble meflin (figure 5k). Although soluble meflin in culture medium repressed TGF-β-induced fibronectin expression in fibroblasts (figure 5l–n), it did not lead to inhibition of the induction of fibronectin expression or restore repression of E-cadherin expression in TGF-β-stimulated MLE-12 cells (figure 5o–s).

Discussion

Fibroblasts are central to the progression of lung fibrosis as represented by excessive production of ECM and aberrant tissue contractility [29, 30]. Our unbiased analysis of scRNA-seq data was performed on a larger cohort, including 32 IPF patients and 29 control subjects, compared with the previous studies [21, 31]. Assessment of the scRNA-seq data from a total of more than 24000 lung cells successfully revealed UMAP-based clustering into six distinct groups. In our analysis, the cells with ISLR gene expression were substantially classified in the $PDGFRB^{+}$ group involving fibroblasts and myofibroblasts, while there was nil or little expression in other lung cells. In our dual ISH study for ISLR and ACTA2 in human normal lungs, very few fibroblasts were positive for ISLR and did not appear to express ACTA2 transcripts, compatible with scRNA-seq analysis. Thus, we identified that the ISLR gene encoding meflin is substantially expressed in fibroblasts of normal lungs as a rare cell population through combined analysis of scRNA-seq and ISH studies.

Fibroblastic foci, active “new” areas of fibrosis, are pathologically found at the interface between normal parenchyma and scarred “old” areas of fibrosis with dense collagen deposition and smooth muscle proliferation [5, 6, 32, 33]. Our data suggest that fibroblasts/myofibroblasts positive for meflin might be closely associated with the pathogenesis for the development of fibroblastic foci, active “new” areas of fibrosis, in IPF. While there is no completely satisfactory animal model of human IPF, the BLM-induced model is relatively well characterised and does exhibit certain features also found in human disease [18–20]. The numbers of fibroblasts positive for meflin increased in the fibrotic lesions of BLM-induced mouse injured lungs as those observed in fibroblastic foci of IPF lungs (figures 2m and 3h). Although recent studies suggested that fibroblasts with meflin expression inhibit not only tumour progression as cancer-associated fibroblasts but also the development of cardiac fibrosis as cardiac fibroblasts [34, 35], there has been little understanding or characterisation of fibroblasts positive for meflin in normal and fibrotic lungs [22]. The BLM-induced meflin KO mice model reveals that meflin-positive fibroblasts have anti-fibrotic properties that prevent exacerbation of local microinjuries and consequently fibrosis. These findings might provide the basis to identify the underlying mechanisms by which meflin-expressing fibroblasts emerge in fibrotic foci, not dense fibrosis, of IPF lungs. In this study, it was hard to determine whether meflin expression might be associated with clinical parameters, including the fibrotic findings evaluated by thin-section computed tomography (TSCT), possibly due to the relatively small numbers of patients (10 IPF patients). Although it remains difficult to distinguish fibrotic foci from dense fibrosis in IPF lungs using TSCT scanning [36–38], our study demonstrated that soluble meflin could be detected in BAL supernatants in parallel with fibrotic activity of BLM-induced lung fibrosis. It encourages us to estimate soluble meflin in BAL supernatants as a biomarker of disease activity in IPF lungs. Although aberrant epithelial–fibroblast communication with activated TGF-β signalling might be assumed to be the pathogenesis of pulmonary fibrosis [3, 33], soluble meflin did not appear to inhibit TGF-β-induced fibrogenesis in epithelial cells *in vitro*.

Cellular senescence has been recently implicated in the pathogenesis of fibrosis [4, 25]. Although senescent fibroblasts were shown to exacerbate fibrogenesis through secretion of SASP factors [4, 26, 27, 39], the secretome of senescent epithelial cells might not activate a fibrogenic response in fibroblasts [4]. Moreover, recent studies showed that TGF-β stimulation might induce cellular senescence [25, 40]. Our data demonstrate that fibroblasts positive for meflin negatively regulate TGF-β-induced cellular senescence and

fibrogenesis. Although TGF-β repressed meflin expression in primary WT fibroblasts, the lack of or repression of meflin in fibroblasts yielded TGF-β-induced cellular senescence [26, 27]. The induction of autocrine TGF-β transcript expression by paracrine TGF-β1 stimulation was augmented in primary meflin KO fibroblasts. Consequently, ECM production and increased α-SMA expression were accelerated in meflin KO fibroblasts *via* paracrine and autocrine TGF-β stimulation [4, 25–27, 39]. The exact mechanism by which meflin regulates TGF-β-induced cell senescence and fibrogenesis has not been fully determined [22, 41]. Nevertheless, the reconstitution of meflin in primary KO fibroblasts blunted TGF-β-induced cell senescence with SASP, followed by the repression of TGF-β-induced fibrogenesis. Furthermore, the induction of meflin into human lung fibroblasts repressed *de novo* fibronectin, α-SMA and collagen expression with Smad activation induced by TGF-β. Our findings provide evidence with which to determine the biological importance of meflin expression on TGF-β-induced cell senescence and fibrogenesis in fibroblasts and myofibroblasts. Furthermore, the targeting of TGF-β signalling was demonstrated to reduce the development of senescence, and improved survival in a mouse model of acute liver injury and failure [25]. Thus, further investigation is warranted to explore how to approach the enhancement of meflin expression on fibroblasts and myofibroblasts in the active fibrotic region of pulmonary fibrosis.

In summary, three remarkable findings are highlighted (figure 6). A new therapeutic strategy for pulmonary fibrosis might be warranted according to the data showing the repressive effect of meflin reconstitution into fibroblasts against TGF-β-induced fibrogenesis and cell senescence.

Acknowledgements: We are indebted to all patients and control subjects who participated in this study.

Author contributions: Y. Nakahara, N. Hashimoto and K. Sakamoto developed the concept and design of the study. Y. Nakahara, N. Hashimoto, K. Sakamoto, N. Omote, A. Ando, K. Wakahara, A. Suzuki, M. Inoue, A. Hara and Y. Mizutani acquired data. Y. Nakahara, N. Hashimoto, K. Sakamoto and T.S. Adams provided analyses. Y. Nakahara, N. Hashimoto and K. Sakamoto were involved in interpretation of data. T. Yokoi performed pathological assessment. A. Enomoto, T.S. Adams, S. Poli, I.O. Rosas and N. Kaminski provided essential material. Y. Nakahara and N. Hashimoto wrote the manuscript. M. Takahashi, K. Imaizumi, T. Kawabe, I.O. Rosas, N. Kaminski and Y. Hasegawa contributed to scientific discussion. All authors reviewed and approved the manuscript.

Conflict of interest: Y. Nakahara has nothing to disclose. N. Hashimoto received a research grant from Boehringer Ingelheim, outside the submitted work. K. Sakamoto has nothing to disclose. A. Enomoto has nothing to disclose. T.S. Adams is an inventor on a provisional patent application (62/849,644) that covers methods related to IPF-associated cell subsets. T. Yokoi has nothing to disclose. N. Omote has nothing to disclose. S. Poli is an inventor on a provisional patent application (62/849,644) that covers methods related to IPF-associated cell subsets. A. Ando has nothing to disclose. K. Wakahara has nothing to disclose. A. Suzuki has nothing to disclose. M. Inoue has nothing to disclose. A. Hara has nothing to disclose. Y. Mizutani has nothing to disclose. K. Imaizumi has nothing to disclose. T. Kawabe has nothing to disclose. I.O. Rosas is an inventor on a provisional patent application (62/849,644) that covers methods related to IPF-associated cell subsets. M. Takahashi has nothing to disclose. N. Kaminski served as a consultant to Biogen Idec, Boehringer Ingelheim, Third Rock, Pliant, Samumed, NuMedii, Indaloo, Theravance, LifeMax, Three Lake Partners and Optikira over the last 3 years and received nonfinancial support from MiRagen; and is an inventor on a provisional patent application (62/849,644) that covers methods related to IPF-associated cell subsets. Y. Hasegawa has nothing to disclose.

Support statement: This work was supported by Grant-in-Aid for Young Scientists (B) (18K15948) to K. Sakamoto, AMED-CREST (Japan Agency for Medical Research and Development, Core Research for Evolutional Science and Technology; 20gm1210009s0102 and 20gm0810007h0105) to A. Enomoto and M. Takahashi, Grant-in-Aid for challenging Exploratory Research (20K21599) to N. Hashimoto, CREST (Core Research for Evolutional Science and Technology; JPMJCR17H3) to N. Hashimoto, and the 24th Promotion Fund of the Annual Meeting of the Medical Society of Japan Commemorative Medicine to N. Hashimoto. This work was also supported by NIH grants R01 HL127349, U01 HL145567, U01 HL122626 and U54 HG008540 to N. Kaminski, NHLBI grant P01 HL114501 and support from the Pulmonary Fibrosis Fund to I.O. Rosa, and an unrestricted gift from Three Lake Partners to I.O. Rosa and N. Kaminski. Funding information for this article has been deposited with the Crossref Funder Registry.

References

1 Lederer DJ, Martinez FJ. Idiopathic pulmonary fibrosis. *N Engl J Med* 2018; 378: 1811–1823.
2 du Bois RM. An earlier and more confident diagnosis of idiopathic pulmonary fibrosis. *Eur Respir Rev* 2012; 21: 141–146.

3 Mora AL, Rojas M, Pardo A, *et al.* Emerging therapies for idiopathic pulmonary fibrosis, a progressive age-related disease. *Nat Rev Drug Discov* 2017; 16: 755–772.
4 Schafer MJ, White TA, Iijima K, *et al.* Cellular senescence mediates fibrotic pulmonary disease. *Nat Commun* 2017; 8: 14532.
5 King TE Jr, Schwarz MI, Brown K, *et al.* Idiopathic pulmonary fibrosis: relationship between histopathologic features and mortality. *Am J Respir Crit Care Med* 2001; 164: 1025–1032.
6 Nicholson AG, Fulford LG, Colby TV, *et al.* The relationship between individual histologic features and disease progression in idiopathic pulmonary fibrosis. *Am J Respir Crit Care Med* 2002; 166: 173–177.
7 Katzenstein AL, Myers JL. Idiopathic pulmonary fibrosis: clinical relevance of pathologic classification. *Am J Respir Crit Care Med* 1998; 157: 1301–1315.
8 Thannickal VJ, Toews GB, White ES, *et al.* Mechanisms of pulmonary fibrosis. *Annu Rev Med* 2004; 55: 395–417.
9 Wynn TA. Integrating mechanisms of pulmonary fibrosis. *J Exp Med* 2011; 208: 1339–1350.
10 Hashimoto N, Jin H, Liu T, *et al.* Bone marrow-derived progenitor cells in pulmonary fibrosis. *J Clin Invest* 2004; 113: 243–252.
11 Hashimoto N, Phan SH, Imaizumi K, *et al.* Endothelial–mesenchymal transition in bleomycin-induced pulmonary fibrosis. *Am J Respir Cell Mol Biol* 2010; 43: 161–172.
12 Rock JR, Barkauskas CE, Cronce MJ, *et al.* Multiple stromal populations contribute to pulmonary fibrosis without evidence for epithelial to mesenchymal transition. *Proc Natl Acad Sci USA* 2011; 108: E1475–E1483.
13 Ubil E, Duan J, Pillai IC, *et al.* Mesenchymal–endothelial transition contributes to cardiac neovascularization. *Nature* 2014; 514: 585–590.
14 Xie T, Liang J, Liu N, *et al.* Transcription factor TBX4 regulates myofibroblast accumulation and lung fibrosis. *J Clin Invest* 2016; 126: 3063–3079.
15 Grun D, van Oudenaarden A. Design and analysis of single-cell sequencing experiments. *Cell* 2015; 163: 799–810.
16 Montoro DT, Haber AL, Biton M, *et al.* A revised airway epithelial hierarchy includes CFTR-expressing ionocytes. *Nature* 2018; 560: 319–324.
17 Plasschaert LW, Zilionis R, Choo-Wing R, *et al.* A single-cell atlas of the airway epithelium reveals the CFTR-rich pulmonary ionocyte. *Nature* 2018; 560: 377–381.
18 Zepp JA, Zacharias WJ, Frank DB, *et al.* Distinct mesenchymal lineages and niches promote epithelial self-renewal and myofibrogenesis in the lung. *Cell* 2017; 170: 1134–1148.
19 Xie T, Wang Y, Deng N, *et al.* Single-cell deconvolution of fibroblast heterogeneity in mouse pulmonary fibrosis. *Cell Rep* 2018; 22: 3625–3640.
20 Peyser R, MacDonnell S, Gao Y, *et al.* Defining the activated fibroblast population in lung fibrosis using single cell sequencing. *Am J Respir Cell Mol Biol* 2019; 61: 74–85.
21 Reyfman PA, Walter JM, Joshi N, *et al.* Single-cell transcriptomic analysis of human lung provides insights into the pathobiology of pulmonary fibrosis. *Am J Respir Crit Care Med* 2019; 199: 1517–1536.
22 Maeda K, Enomoto A, Hara A, *et al.* Identification of meflin as a potential marker for mesenchymal stromal cells. *Sci Rep* 2016; 6: 22288.
23 Adams TS, Schupp JC, Poli S, *et al.* Single-cell RNA-seq reveals ectopic and aberrant lung-resident cell populations in idiopathic pulmonary fibrosis. *Sci Adv* 2020; 6: eaba1983.
24 Sakamoto K, Hashimoto N, Kondoh Y, *et al.* Differential modulation of surfactant protein D under acute and persistent hypoxia in acute lung injury. *Am J Physiol Lung Cell Mol Physiol* 2012; 303: L43–L53.
25 Bird TG, Muller M, Boulter L, *et al.* TGFbeta inhibition restores a regenerative response in acute liver injury by suppressing paracrine senescence. *Sci Transl Med* 2018; 10: eaan1230.
26 Coppe JP, Patil CK, Rodier F, *et al.* Senescence-associated secretory phenotypes reveal cell-nonautonomous functions of oncogenic RAS and the p53 tumor suppressor. *PLoS Biol* 2008; 6: 2853–2868.
27 Coppe JP, Desprez PY, Krtolica A, *et al.* The senescence-associated secretory phenotype: the dark side of tumor suppression. *Annu Rev Pathol* 2010; 5: 99–118.
28 Sheppard D. Pulmonary fibrosis: a cellular overreaction or a failure of communication? *J Clin Invest* 2001; 107: 1501–1502.
29 Herrera J, Henke CA, Bitterman PB. Extracellular matrix as a driver of progressive fibrosis. *J Clin Invest* 2018; 128: 45–53.
30 Lynch MD, Watt FM. Fibroblast heterogeneity: implications for human disease. *J Clin Invest* 2018; 128: 26–35.
31 Xu Y, Mizuno T, Sridharan A, *et al.* Single-cell RNA sequencing identifies diverse roles of epithelial cells in idiopathic pulmonary fibrosis. *JCI Insight* 2016; 1: e90558.
32 Smith M, Dalurzo M, Panse P, *et al.* Usual interstitial pneumonia-pattern fibrosis in surgical lung biopsies. Clinical, radiological and histopathological clues to aetiology. *J Clin Pathol* 2013; 66: 896–903.
33 Richeldi L, Collard HR, Jones MG. Idiopathic pulmonary fibrosis. *Lancet* 2017; 389: 1941–1952.
34 Hara A, Kobayashi H, Asai N, *et al.* Roles of the mesenchymal stromal/stem cell marker meflin in cardiac tissue repair and the development of diastolic dysfunction. *Circ Res* 2019; 125: 414–430.

35 Mizutani Y, Kobayashi H, Iida T, *et al.* Meflin-positive cancer-associated fibroblasts inhibit pancreatic carcinogenesis. *Cancer Res* 2020; 79: 5367–5381.

36 Hashimoto N, Ando A, Iwano S, *et al.* Thin-section computed tomography-determined usual interstitial pneumonia pattern affects the decision-making process for resection in newly diagnosed lung cancer patients: a retrospective study. *BMC Pulm Med* 2018; 18: 2.

37 Luzina IG, Salcedo MV, Rojas-Pena ML, *et al.* Transcriptomic evidence of immune activation in macroscopically normal-appearing and scarred lung tissues in idiopathic pulmonary fibrosis. *Cell Immunol* 2018; 325: 1–13.

38 McDonough JE, Ahangari F, Li Q, *et al.* Transcriptional regulatory model of fibrosis progression in the human lung. *JCI Insight* 2019; 4: e131597.

39 Alvarez D, Cardenes N, Sellares J, *et al.* IPF lung fibroblasts have a senescent phenotype. *Am J Physiol Lung Cell Mol Physiol* 2017; 313: L1164–L1173.

40 Rapisarda V, Borghesan M, Miguela V, *et al.* Integrin beta 3 regulates cellular senescence by activating the TGF-beta pathway. *Cell Rep* 2017; 18: 2480–2493.

41 Nagasawa A, Kubota R, Imamura Y, *et al.* Cloning of the cDNA for a new member of the immunoglobulin superfamily (ISLR) containing leucine-rich repeat (LRR). *Genomics* 1997; 44: 273–279.